
Long-Term Effects of “Ecstasy” Use on Serotonin Transporters of the Brain Investigated by PET

Ralph Buchert, PhD¹; Rainer Thomasius, MD²; Bruno Nebeling, PhD¹; Kay Petersen, PhD²; Jost Obrocki, MD²; Lars Jenicke, MD¹; Florian Wilke¹; Lutz Wartberg²; Pavlina Zapletalova, MS²; and Malte Clausen, MD¹

¹Department of Nuclear Medicine, University Hospital Hamburg-Eppendorf, Hamburg, Germany; and ²Department of Psychiatry and Psychotherapy, University Hospital Hamburg-Eppendorf, Hamburg, Germany

Alterations of the serotonergic system due to ecstasy consumption have been extensively documented in recent literature. However, reversibility of these neurotoxic effects still remains unclear. To address this question, PET was performed using the serotonin transporter (SERT) ligand ¹¹C-(+)-McN5652 in a total of 117 subjects subdivided into 4 groups: actual ecstasy users (*n* = 30), former ecstasy users (*n* = 29), drug-naive control subjects (*n* = 29), and subjects with abuse of psychoactive agents other than ecstasy (*n* = 29). **Methods:** About 500 MBq ¹¹C-(+)-McN5652 were injected intravenously. Thirty-five scans were acquired according to a dynamic scan protocol of 90 min using a full-ring whole-body PET system. Transaxial slices were reconstructed using an iterative method. Individual brains were transformed to a template defined earlier. Distribution volume ratios (DVRs) were derived by application of a reference tissue approach for reversible binding. Gray matter of the cerebellum served as reference. SERT-rich brain regions—mesencephalon, putamen, caudate, and thalamus—were selected for the evaluation of SERT availability using volumes of interest predefined in the template. **Results:** Compared with drug-naive control subjects, the DVR in actual ecstasy users was significantly reduced in the mesencephalon (*P* = 0.004) and the thalamus (*P* = 0.044). The DVR in former ecstasy users was very close to the DVR in drug-naive control subjects in all brain regions. The DVR in polydrug users was slightly higher than that in the drug-naive control subjects in all SERT-rich regions (not statistically significant). **Conclusion:** Our findings further support the hypothesis of ecstasy-induced protracted alterations of the SERT. In addition, they might indicate reversibility of the availability of SERT as measured by PET. However, this does not imply full reversibility of the neurotoxic effects.

Key Words: ecstasy; long-term effects; serotonin transporter; PET; ¹¹C-(+)-McN5652

J Nucl Med 2003; 44:375–384

Received May 2, 2002; revision accepted Sep. 25, 2002.
For correspondence or reprints contact: Ralph Buchert, PhD, Department of Nuclear Medicine, University Hospital Hamburg-Eppendorf, Martinistrasse 52, D-20246 Hamburg, Germany.
E-mail: buchert@uke.uni-hamburg.de

The synthetic hallucinogen, 3,4-methylenedioxymethamphetamine (MDMA) is the main psychoactive constituent of the popular recreational drug ecstasy. It produces euphoria, increase in psychomotor drive, and enhanced sociability. Because of these effects, ecstasy has become popular among adolescents and young adults.

However, apart from these psychologic effects, there is increasing evidence for the neurotoxicity of MDMA (1). Initial findings in animals (in both rats and nonhuman primates) indicated that MDMA might cause alterations of serotonergic neurons in the brain (2–5). Moreover, significantly reduced concentrations of 5-hydroxyindoleacetic acid in the cerebrospinal fluid in human ecstasy users gave evidence that MDMA also leads to an impairment of serotonin neurons in the human brain (6).

To further explore the effect of MDMA on the serotonergic system, markers of the presynaptic serotonin transporter (SERT) have been developed. Using PET, Szabo et al. (7) demonstrated high specific ligand binding of ¹¹C-(+)-McN5652 to SERT of the human brain in vivo. Initial investigations of specific ¹¹C-(+)-McN5652 binding in MDMA users were performed by McCann et al. (8). In 14 previous ecstasy users, a decreased global and local binding to SERT was observed compared with that of 15 control subjects who had never used MDMA. Ecstasy users had abstained from psychoactive drugs for 19 wk (range, 3–147 wk) before the study. Semple et al. (9), using ¹²³I-2β-carbomethoxy-3β-(4-fluorophenyl)tropane (¹²³I-β-CIT) SPECT, detected a cortical reduction of cerebral SERTs in long-term MDMA users compared with MDMA-naive but other drug-using subjects. In ecstasy users, SPECT was performed 2.6 ± 1.1 wk (range, 0.9–4.0 wk) after the last tablet. In a study of cerebral glucose metabolism using PET with ¹⁸F-FDG, local uptake of ¹⁸F-FDG was reduced within the striatum and the amygdala in 93 ecstasy users compared with that of 27 control subjects (10,11). The time since the last ecstasy ingestion on the day of PET was 28 ± 62 wk (range, 0.4–416 wk).

TABLE 1
Demographics

Parameter	Actual ecstasy users (group A)	Former ecstasy users (group F)	Drug-naive controls (group N)	Polydrug users (group P)
<i>n</i>	30	29	29	29
Age (y)	24.5 ± 4.2 (19–34)	24.2 ± 3.6 (19–36)	23.3 ± 3.7 (18–33)	24.4 ± 4.6 (18–35)
Sex (F/M)	15/15	14/15	15/14	14/15

Data are given as mean ± 1 SD (range).

However, it is still unclear whether MDMA leads to an irreversible impairment of serotonergic neurons or whether neuronal alterations are reversible after withdrawing from using ecstasy. Moreover, criticism of previous studies concerned the potential concurrent abuse of psychoactive agents other than ecstasy that might also cause a reduction of the availability of SERT.

Therefore, the aim of this study was to investigate the long-term effect of MDMA use on the serotonergic system by ¹¹C-(+)-McN5652 PET in a rather large number of subjects with special regard for actual or former ecstasy abuse and abuse of psychoactive substances other than MDMA.

MATERIALS AND METHODS

Subjects

PET using the SERT ligand ¹¹C-(+)-McN5652 (12) was performed on 120 healthy subjects without psychiatric history divided into 4 different groups: actual ecstasy users (group A), former ecstasy users (group F), subjects without any known history of illicit-drug abuse (drug-naive, group N), and subjects with abuse of psychoactive agents other than ecstasy (polydrug users, group P). All subjects were tested for psychopathology with the Structured Clinical Interview for DSM-IV (SKID) (13). Subjects currently suffering from any axis I disorder, except substance-related disorders (not alcohol- or opiate-related disorders), were excluded from the study. Drug history was ascertained by a standardized questionnaire. Plausibility of the drug users' self-assessment was verified by testing of hair samples. Participants abstained from use of all psychoactive drugs for at least 3 d before the study. To verify this abstinence period, the urine of all subjects was screened for the presence of amphetamines, barbiturates, benzodiazepines, canna-

binoids, cocaine metabolites, opiates, and alcohol on the day of PET. Subjects who tested positive for any of these substance groups, except cannabinoids, were excluded from the study. However, urine testing results might be false-positive. Therefore, in 3 subjects with authentic self-assessment, PET was performed despite positive urine screening. In these subjects an additional blood screening for drugs was performed. The positive urine test was confirmed by blood screening in 2 of these subjects, which led to the exclusion from the study after PET scanning. Thus, the abstinence period was verified in all subjects included in the study. Scanning of 1 further subject could not be completed because of claustrophobia. Demographic data of the remaining 117 subjects are given in detail in Table 1.

The study was approved by the local ethics committee and radiation protection authorities. All participants gave their written informed consent.

Actual Ecstasy Users (Group A). Thirty actual ecstasy users (15 females, 15 males; mean age, 24.5 ± 4.2 y) were investigated. Inclusion criterion was regular ecstasy use (at least once per week) of at least 2 tablets within 48 h each time. Drug-history data are listed in detail in Tables 2 and 3.

Former Ecstasy Users (Group F). Twenty-nine former ecstasy users (14 females, 15 males; mean age, 24.2 ± 3.6 y) were investigated. The inclusion criterion was a cumulative ecstasy dose of at least 250 tablets and 400 tablets in female and male subjects, respectively. We included those subjects who took ecstasy for at least 36 mo with the last MDMA ingestion at least 20 wk before ¹¹C-(+)-McN5652 PET. Drug-history data are listed in detail in Tables 2 and 3.

Drug-Naive Subjects (Group N). Twenty-nine subjects (15 females, 14 males; mean age, 23.3 ± 3.7 y) without any known history of illicit drug abuse served as the control group. Drug-naive control subjects were not on any psychoactive medication. Use of alcohol or nicotine that did not fulfill the dependence criteria

TABLE 2
Ecstasy Consumption Data

Parameter	Actual ecstasy users (group A)	Former ecstasy users (group F)
Cumulated ecstasy dose (tablets)	827 ± 1,268 (13–6,873)	793 ± 679 (78–3,122)
Duration of use (mo)	54 ± 32 (5–120)	55 ± 27 (18–116)
Time since last ecstasy ingestion at day of PET (d)	24 ± 16 (4–60)	514 ± 472 (90–1,500)
Age at first ecstasy ingestion (y)	20.0 ± 3.8 (14–30)	18.3 ± 3.0 (15–28)

Data are given as mean ± 1 SD (range).

TABLE 3
Exposure to Drugs Other than Ecstasy

Parameter	Actual ecstasy users (group A)	Former ecstasy users (group F)	Drug-naïve controls (group N)	Polydrug users (group P)
Amphetamine cumulated dose (g)	68 ± 106	77 ± 115	0	4 ± 9
Cannabis cumulated dose (g)	567 ± 1,188	2,133 ± 2,200	0	1,232 ± 1,303
LSD cumulated dose (g)	1.6 ± 5.2	2.4 ± 5.1	0	0.2 ± 0.4
Psilocybine cumulated dose (g)	0.9 ± 3.2	5.1 ± 15.6	0	14.4 ± 32.5
Cocaine cumulated dose (g)	38 ± 75	101 ± 219	0	255 ± 708
Alcohol in past week (g)	94 ± 97	152 ± 198	71 ± 72	197 ± 195
Nicotine in past week (cigarettes)	53 ± 58	101 ± 71	66 ± 65	135 ± 80

LSD = lysergic acid diethylamide.
Data are given as mean ± 1 SD.

according to the *Diagnostic and Statistical Manual of Mental Disorders* (DSM) (14) was no exclusion criterion.

Polydrug Users (Group P). Twenty-nine subjects (14 females, 15 males; mean age, 24.4 ± 4.6 y) with abuse of psychoactive substances other than ecstasy were investigated. Drug abuse in this group was intended to match drug abuse in the ecstasy consumer groups, except ecstasy. The last drug ingestion was from at least 3 d to a maximum of 2 wk before ¹¹C-(+)-McN5652 PET. Data concerning illicit-drug abuse are listed in detail in Tables 2 and 3.

¹¹C-(+)-McN5652

The parent compound of the radiotracer, McN5652-z (6-[4-methylthiophenyl]-1,2,3,5,6,10b-hexahydropyrrolo[2,1-a]isoquinoline), was synthesized and fully determined by x-ray structural analysis and nuclear magnetic resonance spectroscopy (nuclear Overhauser effect measurements). The 2 diastereomers were unequivocally assigned and compared with an authentic sample. Because this compound possesses 2 centers of asymmetry, there are 4 stereoisomers (6*S*, 10*bR*), (6*R*, 10*bS*), (6*S*, 10*bS*), and (6*R*, 10*bR*). Regarding the position of the hydrogen atoms at C-6 and C-10b, the 2 enantiomeric pairs were called *cis* and *trans*. The diastereoisomers were separated by preparative column chromatography, and the previously described (+)-enantiomer was separated by semipreparative chromatography on a chiral phase (amylose tris[3,5-dimethylphenyl carbamat]) and compared with an authentic sample of the (+)-McN5652-z enantiomer (15).

To generate the precursor for the labeling with ¹¹C-methyl iodide, the (+)-McN5652-z enantiomer was demethylated and the corresponding thiolate was isolated with a chemical purity of 98.5% using solid-phase extraction techniques. The precursor was fractionated in quantities of 200 μg and stored at -80°C.

The labeling of the thiolate with ¹¹C-CH₃I, which was first generated by classical reduction of ¹¹C-CO₂, resulted in an average specific activity of 45 MBq/nmol for ¹¹C-(+)-McN5652-z at the end of synthesis. An improvement of the average specific activity by a factor of 10 was achieved when generating the ¹¹C-CH₃I by direct iodination of the in-target produced, ¹¹C-CH₄. The synthesis time was 22 min. The radiochemical yield was 14% ± 5%.

The purity of the enantiomer, radionuclidic purity, and radiochemical purity were more than 99.5%, 99.9%, and 90.0%, respectively. The radiochemical purity was limited because of the decomposition of the ¹¹C-(+)-McN5652-z depending on the amount of activity produced. The specific activity at the end of synthesis was >30 MBq/nmol (mean ± 1 SD, 177 ± 108 MBq/nmol; range, 30–537 MBq/nmol). Doses dispensed to the participants are summarized in Table 4.

PET

PET was performed on a full-ring, whole-body ECAT EXACT 921/47 system (Siemens/CTI, Knoxville, TN) in 2-dimensional mode. This system covers an axial field of view of 16.2 cm by collecting 47 transversal slices with 3.4-mm slice separation.

Head movement minimization was achieved by a thermoplastic mask immobilization system (Tru-Scan Imaging, Annapolis, MD). A 15-min transmission scan for attenuation correction was obtained before tracer injection using 3 rotating ⁶⁸Ge rod sources, about 70 MBq each. After obtaining the transmission scan, 466 ± 76 MBq ¹¹C-(+)-McN5652, dissolved in 40 mL 0.9% NaCl, were injected through a vein of the left hand at a flow rate of 600 mL/h. Thus, the total infusion time was 4 min. At the beginning of tracer injection a dynamic scan protocol was initiated, including 35 frames with a total acquisition time of 90 min (9 × 20 s, 6 × 30 s,

TABLE 4
Injected Tracer Doses

Parameter	Actual ecstasy users (group A)	Former ecstasy users (group F)	Drug-naïve controls (group N)	Polydrug users (group P)
Radioactivity dose (MBq)	465 ± 87 (324–700)	451 ± 71 (251–549)	467 ± 84 (134–582)	480 ± 59 (360–555)
Specific activity at injection (MBq/nmol)	56.4 ± 50.0 (14.0–203)	66.5 ± 47.5 (14.6–204)	87.7 ± 44.0 (14.7–175)	120 ± 56.7 (47.4–302)
Mass dose (nmol)	14.9 ± 9.8 (1.6–35.3)	11.2 ± 8.6 (2.3–35.2)	8.0 ± 7.7 (2.2–36.7)	4.7 ± 1.7 (1.3–8.6)

Data are given as mean ± 1 SD (range).

4 × 60 s, 5 × 120 s, 8 × 300 s, and 3 × 600 s). Subjects were asked to keep their eyes open during the entire time of acquisition. Noise in the acquisition room was kept to a minimum.

The sinograms were corrected for random coincidences, radioactive decay, dead time, and varying detector efficiency. Thereafter, sinograms were 3-dimensionally smoothed by application of a 3 × 3 × 3 binomial kernel (smoother software, J. van den Hoff, Medical University, Hannover, Germany). Forty-seven transaxial slices with 64 × 64 voxels were reconstructed using an iterative method (ira-1.25 software, H. Fricke, Medical University, Hannover, Germany) (order-subsets expectation maximization [OSEM], 24 subsets, 3 iterations). The voxel size was 3.4 × 3.4 × 3.4 mm³; in-plane spatial resolution was about 9-mm full width at half maximum (FWHM). No scatter correction was performed.

Data Preprocessing

For further processing, the format of the reconstructed images was converted from the scanner-specific ECAT 6.5 format to ANALYZE format using the commercial PMOD software package (Version 2.25 for Windows NT; Medical Imaging Software, Zurich, Switzerland) (16). Then the images were flipped top to bottom and the 4-dimensional dataset was clipped to thirty-five 3-dimensional datasets, each 3-dimensional dataset containing 1 single frame of the dynamic study (MRicro 1.30, Chris Rorden, University of Nottingham, Nottingham, U.K.) (17).

To correct the remaining head movement, frames 12–35 (4–90 min after injection) were coregistered using the Realign-Tool of the SPM99 software package (Wellcome Department of Cognitive Neurology, Institute of Neurology, University College London, London, U.K.) (18) (parameter values: coregister only; always mask images; registration quality 0.5; don't allow weighting of reference image). Frame 27 (30–35 min after injection) served as the reference frame for coregistration. Because frames 1–11 did not provide sufficient anatomic information for the convergence of the realign algorithm, the transformation matrix for frame 12 was applied to these frames assuming that there was no relevant movement during the first 4 min of the acquisition.

To support standardized identification of the volumes of interest (VOIs) in each subject, individual images were stereotactically normalized using the Normalize-Tool of SPM99 (parameter values for nonlinear warping: 7 × 8 × 7 nonlinear basis functions; 12 nonlinear iterations; medium nonlinear regularization; default brain mask; don't mask object). To determine the normalization parameters, the summed image of frames 27–35 (30–90 min after injection) was compared with a template defined earlier (mean of 9 summed ¹¹C-(+)-McN5652 PET scans acquired during a pilot study). Realignment and normalization were combined to 1 single transformation. Transformed images were written with a voxel size of 3 × 3 × 3 mm³ using sinc interpolation.

After motion correction and stereotactic normalization, the thirty-five 3-dimensional datasets were reconverted to a single 4-dimensional dataset using MRicro. Finally, the quality of the preprocessing steps was controlled by visual inspection of the 4-dimensional dataset in cine mode and by comparing the normalized individual summed image and the template using corresponding crosshairs.

VOIs

According to the current literature, the following brain structures were selected for testing the hypothesis of ecstasy-induced

alteration of SERT availability (19–21): mesencephalon, putamen, caudate, and thalamus. The white matter served as the control region in which no ecstasy-induced effects were expected because of the absence of SERT. The gray matter of the cerebellum was chosen as the reference region for the kinetic modeling.

VOIs for the structures to be examined were predefined in the template. Each VOI was composed of circles of 4.1 mm in radius, placed in an appropriate number of transversal slices using the VOI-Tool of PMOD (Fig. 1) (22). No individual adjustment was performed to guarantee reproducible results. However, in 3 subjects the cerebellum was partly outside of the field of view of the PET scanner, so that the cerebellum VOI had to be adjusted manually.

Kinetic Modeling

Modeling was performed on the level of voxels. Distribution volume ratios (DVRs) were derived by application of the graphic reference tissue method for reversible binding described by Ichise et al. (23) (Ichise noninvasive plot).

The Ichise noninvasive plot is easily derived from the more widely known invasive Logan plot for the graphical analysis of reversible radioligand binding (24). The operational equation of the Logan plot reads:

$$\frac{\int_0^t C(s)ds}{C(t)} \approx DV \times \frac{\int_0^t C_p(s)ds}{C(t)} + b, \quad t > t^*, \quad \text{Eq. 1}$$

where C(t) is the time–activity curve of a tissue voxel or VOI, C_p(t) is the time–activity curve of the free fraction of unmetabolized tracer in arterial plasma (input function), DV is the total distribution volume of the tracer in the tissue, and b is a quantity that becomes constant at late times t > t*. DV is defined as the tissue-to-plasma ratio C/C_p at equilibrium. Neglecting fractional blood volume DV is just the sum of the nondisplaceable and the specific distribution volume—that is:

$$DV = DV_{\text{nondispl}} + DV_{\text{spec}}. \quad \text{Eq. 2}$$

Now, combining the Logan plot formula (Eq. 1) for 2 different tissue time–activity curves, C and C_r, by solving the C_r formula for the plasma integral and inserting the result in the C formula yields:

$$\frac{\int_0^t C(s)ds}{C(t)} \approx \text{DVR} \times \frac{\int_0^t C_r(s)ds}{C(t)} - \text{DVR} \times b_r \times \frac{C_r(t)}{C(t)} + b, \quad t > t^*, \quad \text{Eq. 3}$$

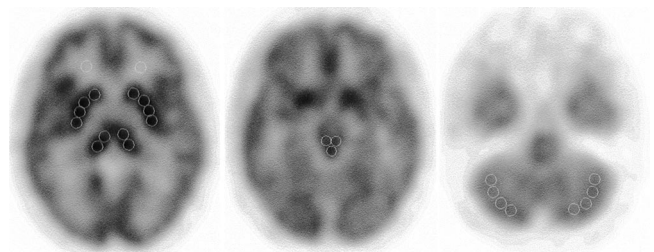


FIGURE 1. Definition of VOIs for putamen, caudate, thalamus, and white matter (left), mesencephalon (middle), and cerebellum (right) in transversal slices of the ¹¹C-(+)-McN5652-PET template. VOIs were composed of circles of 4.1-mm radius drawn in appropriate number of slices (mesencephalon, no. of slices = 3/no. of circles = 9/no. of voxels = 50; putamen, 4/24/166; caudate, 6/12/83; thalamus, 4/16/105; cerebellum, 5/40/273; white matter, 8/16/108).

where DVR is the distribution volume ratio:

$$\text{DVR} \equiv \frac{\text{DV}}{\text{DV}_r}. \quad \text{Eq. 4}$$

Equation 3 is the operational equation of the Ichise noninvasive plot. Beyond time t^* it is a multilinear equation. Thus, the DVR is easily obtained by multilinear regression analysis.

Assuming that C_r is taken from a reference tissue, which is devoid of the receptor under consideration and provides approximately the same nondisplaceable DV as that of receptor-rich tissue, one obtains from Equations 2 and 4:

$$\text{DVR} \approx 1 + \frac{\text{DV}_{\text{spec}}}{\text{DV}_{\text{nondispl}}}. \quad \text{Eq. 5}$$

The ratio $\text{DV}_{\text{spec}}/\text{DV}_{\text{nondispl}}$ is commonly denoted as binding potential BP^* . It is related to the density of available receptors, B_0 , and the equilibrium dissociation constant, K_d , according to:

$$\text{BP}^* = \frac{B_0}{K_d \times \text{DV}_{\text{nondispl}}}. \quad \text{Eq. 6}$$

Therefore, for the DVR to reflect the receptor density, both, K_d and $\text{DV}_{\text{nondispl}}$ must be constant between individuals and diseases.

The time–activity curve of the reference region was generated using the mean of the cerebellum VOI. The starting time for the multilinear regression analysis was fixed at $t^* = 12$ min.

DVRs for the examined structures were taken to be the mean voxel values within the corresponding VOIs copied to the individual parametric images.

In addition to DVRs, semiquantitative standardized uptake values (SUVs) were considered. To this end, images of tracer uptake were obtained by summing frames 31–35 (50–90 min after injection). SUVs were then computed as the ratio of tracer uptake to injected dose per body weight (kBq/mL/[MBq/kg]).

Statistical Analysis

The following a priori predictions were made:

- H1. Ecstasy use causes long-lasting reduction of SERT availability. This leads to a reduction of the DVR of ^{11}C -(+)-McN5652 in the SERT-rich regions mesencephalon, pu-

tamen, caudate, and thalamus in both former and actual ecstasy users compared with the group of drug-naive control subjects.

- H2. There is no group difference in the DVR in the white matter, which is devoid of SERT.
- H3. There is a difference in the DVR between the group of polydrug users and the group of drug-naive control subjects in the SERT-rich brain regions.

One-way ANOVA and post hoc tests for multiple comparisons were used to test these hypotheses. The Scheffé or Tamhane post hoc test was applied according to the result of the Levene test of homogeneity of variances. These post hoc tests are deliberately conservative to reduce the probability of too many significant differences arising by chance. No additional Bonferroni adjustment for the number of VOIs was performed. All statistic computations were performed using SPSS 10.0 (SPSS, Inc., Chicago, IL) for Microsoft Windows (Redmond, WA).

RESULTS

Representative time–activity curves are shown in Figure 2.

The results of the VOI analysis are listed in detail in Tables 5 and 6. In all SERT-rich regions, the mean DVR was lowest in the group of actual ecstasy users and highest in the group of polydrug users. The mean DVRs in the group of former ecstasy users and in the group of drug-naive control subjects were very similar and slightly lower than that in the group of polydrug users.

ANOVA detected differences in the DVR between the 4 groups to be statistically significant in the mesencephalon (2-tailed $P = 0.000$), caudate ($P = 0.032$), and thalamus ($P = 0.022$). There was no significant difference in the putamen ($P = 0.187$) and white matter ($P = 0.732$). According to the Levene test, variances were homogeneous in all structures. Therefore, the Scheffé test was applied for multiple comparisons in the structures with significant ANOVA. In the mesencephalon, the DVR was significantly smaller in the group of actual ecstasy users than in all other

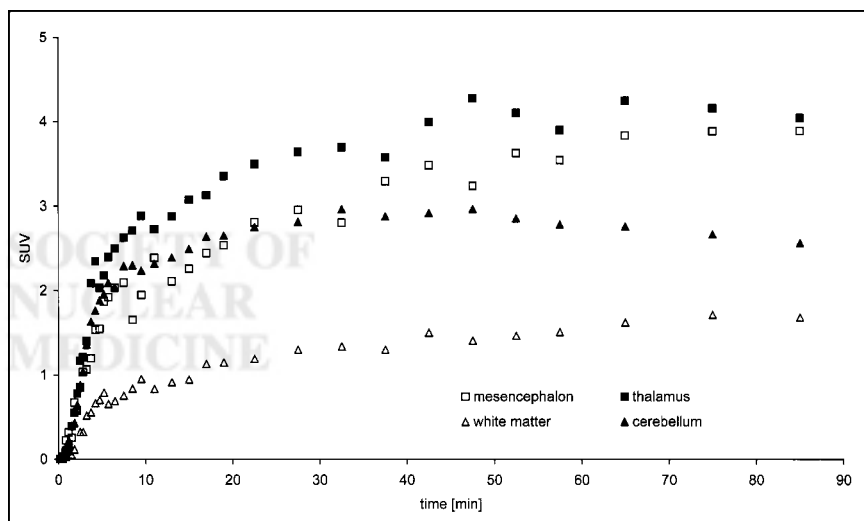


FIGURE 2. Representative time–activity curves. SUVs for mesencephalon, thalamus, white matter, and cerebellum VOIs in drug-naive control subject are plotted.

TABLE 5
DVRs, 1-Way ANOVA, and Scheffé Post Hoc Test

Region	Actual ecstasy users (group A) (n = 30)	Former ecstasy users (group F) (n = 29)	Drug-naïve controls (group N) (n = 29)	Polydrug users (group P) (n = 29)	ANOVA			Scheffé test
					dF	F	P	
Mesencephalon	1.163 ± 0.071	1.220 ± 0.074	1.224 ± 0.047	1.234 ± 0.069	116	6.858	0.000	A/F* A/N* A/P†
Putamen	1.356 ± 0.100	1.386 ± 0.097	1.387 ± 0.066	1.407 ± 0.090	116	1.628	0.187	
Caudate	1.198 ± 0.085	1.239 ± 0.093	1.239 ± 0.049	1.258 ± 0.082	116	3.034	0.032	A/P‡
Thalamus	1.349 ± 0.088	1.402 ± 0.090	1.408 ± 0.073	1.411 ± 0.100	116	3.341	0.022	A/N‡ A/P‡
White matter	0.561 ± 0.064	0.565 ± 0.047	0.577 ± 0.057	0.566 ± 0.062	116	0.430	0.732	

* $P \leq 0.01$ (significance level of 1-tailed Scheffé test).

† $P \leq 0.001$ (significance level of 1-tailed Scheffé test).

‡ $P \leq 0.05$ (significance level of 1-tailed Scheffé test).

DVRs are given as mean ± 1 SD.

groups (1-tailed $P[A/F] = 0.008$, $P[A/N] = 0.004$, $P[A/P] = 0.000$). In the caudate, the DVR was significantly smaller in the group of actual ecstasy users than in the group of polydrug users ($P[A/P] = 0.022$). In the thalamus, the DVR was significantly smaller in the group of actual ecstasy users than in both the group of drug-naïve control subjects and the group of polydrug users ($P[A/N] = 0.044$, $P[A/P] = 0.033$).

The mean SUVs were highest in the group of drug-naïve control subjects in all regions. The mean SUVs in the group of actual ecstasy users and the group of polydrug users were rather similar and were slightly larger than those in the group of former ecstasy users, who showed the smallest SUVs in all regions. ANOVA detected differences in the SUV to be statistically significant only in the white matter VOI. However, the following Scheffé test did not yield a significant result for the difference between the SUV in white matter for any pair of groups.

DISCUSSION

Because the drug ecstasy has become increasingly popular among adolescents and young adults, neurotoxic long-

term effects of recreational use of MDMA are a focus of ongoing research. Criticisms of previous studies are related to the potential overlapping neuronal effects of concurrently used drugs. Furthermore, it remains unclear whether alterations of the serotonergic system are in principle reversible or whether neurotoxic alterations may persist even after stopping MDMA abuse. To address these questions, PET using the SERT ligand ^{11}C -(+)-McN5652 was performed on actual ecstasy users, former ecstasy users, drug-naïve control subjects, and subjects with abuse of psychoactive agents other than ecstasy.

Compared with drug-naïve control subjects, the DVR in actual ecstasy users was reduced in all SERT-rich regions. The reduction was statistically significant in the mesencephalon and thalamus. This result further supports the hypothesis that ecstasy use causes protracted alterations of the brain serotonergic system that last (at least) several weeks (H1).

In the white matter, there were no significant differences in the DVR between the 4 groups. Because the white matter is devoid of SERT, this supports the hypothesis that the

TABLE 6
SUVs, 1-Way ANOVA, and Scheffé Post Hoc Test

Region	Actual ecstasy users (group A) (n = 30)	Former ecstasy users (group F) (n = 29)	Drug-naïve controls (group N) (n = 29)	Polydrug users (group P) (n = 28)	ANOVA			Scheffé test
					dF	F	P	
Mesencephalon	3.856 ± 0.615	3.784 ± 0.929	4.243 ± 0.645	3.861 ± 0.640	115	2.421	0.070	
Putamen	4.173 ± 0.690	4.037 ± 1.030	4.452 ± 0.708	4.144 ± 0.634	115	1.481	0.224	
Caudate	3.663 ± 0.593	3.559 ± 0.921	3.946 ± 0.631	3.567 ± 0.577	115	1.957	0.125	
Thalamus	4.166 ± 0.669	4.095 ± 1.037	4.556 ± 0.729	4.158 ± 0.703	115	2.017	0.116	
White matter	1.914 ± 0.321	1.775 ± 0.374	2.000 ± 0.333	1.789 ± 0.328	115	2.883	0.039	—
Cerebellum	2.797 ± 0.478	2.612 ± 0.600	2.858 ± 0.450	2.612 ± 0.386	115	1.964	0.123	

SUVs are given as mean ± 1 SD.

observed effects in SERT-rich regions indeed indicate differences in SERT availability (H2).

The DVR in former ecstasy users was very close to the DVR in drug-naive control subjects. There was no significant difference between these groups; there was not even a tendency (2-sided $P[F/N] = 0.997$ in mesencephalon). This is in agreement with the results of Reneman et al. (25,26). Using ^{123}I - β -CIT SPECT and the cerebellum as the reference region, this group found no difference in the SERT availability in 16 individuals who stopped using MDMA 29 \pm 20 mo earlier compared with 15 control subjects who had never used MDMA. The potential reversibility of SERT availability was reported by Scheffel et al. (27) using PET with ^{11}C -(+)-McN5652 and, for the estimation of nonspecific binding, its pharmacologically inactive enantiomer ^{11}C -(-)-McN5652 in baboons. Their study showed that SERT binding was reduced in all brain regions 40 d after MDMA ingestion. In contrast, 9- and 13-mo follow-up PET showed recovery of SERTs, however, with regional differences. This again is in good agreement with Semple et al. (9), who reported evidence of recovery from alterations of brain serotonergic neurons after withdraw of MDMA abuse using ^{123}I - β -CIT SPECT and the cerebellum as the reference region. They described a positive partial correlation of relative tracer uptake in many brain regions and the interval since intake of the last tablet in a group of 10 male ecstasy users. Indication that the neuroendocrine impairment caused by MDMA may be due to a partially reversible neurotoxic action was also reported by Gerra et al. (28). In 15 MDMA users, who did not show other drug dependencies or prolonged alcohol abuse, prolactin and cortisol responses to the serotonergic agonist d-fenfluramine were significantly reduced after 3 wk of ecstasy abstinence compared with those of control subjects. Twelve months later, the prolactin response was still reduced but the cortisol response had normalized.

Histologic examination of the brain 5-hydroxytryptamine (5-HT) innervation pattern in MDMA-treated squirrel monkeys revealed a reduced density of serotonergic axons even 7 y after MDMA treatment, although the deficits were less severe than those at 18 mo after the treatment (29). These histologic results are not in conflict with the results of in vivo functional brain imaging cited above. Brain imaging measures the availability of receptors for the ligand used, which not only is a function of receptor density but also depends on the actual affinity of the receptor for the ligand, the transmitter synaptic concentration, and the transmitter receptor occupancy. Thus, in the outcome measures of functional brain imaging, reduced SERT density might be compensated by other effects. In this context, the results of Kish et al. (30), who found 50%–80% reduced striatal 5-HT levels in a postmortem study of a single ecstasy user, may be relevant. Reneman et al. (31) conducted a SPECT study with the ligand ^{123}I -5-I-R91150 for the postsynaptic 5-HT_{2A} receptor. In 5 abstinent MDMA users, the binding ratio of ^{123}I -5-I-R91150 in the occipital cortex was significantly

elevated compared with that of 9 healthy control subjects. This may indicate an upregulation of the postsynaptic 5-HT_{2A} receptor following the lesion of serotonergic afferents. In a second ^{123}I -5-I-R91150 SPECT study, Reneman et al. (32) found that the mean cortical binding ratios were significantly lower in recent MDMA users than in former MDMA users and control subjects. Finally, axonal regeneration may lead to abnormal, dysfunctional circuitry.

Thus, the key question of whether MDMA leads to an irreversible or (partly) reversible impairment of serotonergic neurons remains controversial. To further examine this question, follow-up examinations of MDMA users are currently performed.

Ecstasy users usually take additional psychoactive substances. Therefore, findings of ^{11}C -(+)-McN5652 binding are not necessarily specific—that is, secondary to ecstasy use. In addition, (heavy) users of ecstasy may have different personalities than those of people who have never used drugs. Therefore, this study investigated a second control group of polydrug users who did not use ecstasy but were intended to be matched with the ecstasy users for the consumption of other drugs. We found the DVR in the polydrug users to be slightly higher in all SERT-rich regions, including the mesencephalon, putamen, caudate, and thalamus, than that in the drug-naive control subjects (H3). Nevertheless, the difference was not statistically significant in any region. However, although the reduction of the DVR in the caudate of actual ecstasy users was not statistically significant relative to that of the drug-naive control subjects, it was significant relative to that of the group of polydrug users, despite the fact that the SD was larger in the group of polydrug users than that in the group of drug-naive control subjects in all brain regions. The slightly increased DVR in the group of polydrug users might be explained by acute serotonergic dysfunction during acute abstinence from chronic cocaine use, for example. This effect was described by Jacobsen et al. (33), who found elevated central SERT availability using ^{123}I - β -CIT SPECT in 15 cocaine-dependent subjects who were abstinent from drug use a mean of 3.7 d compared with 37 healthy comparison subjects.

The analysis of SUVs did not reveal any statistically significant results. This might be explained by the rather large variance of SUVs. The relative SD of SUVs within the different VOIs and groups was 15%–27%, whereas it was 4%–7% for the DVRs. However, SUVs were lowest in the group of former ecstasy users in all VOIs. In addition, SUVs in the polydrug control group were quite similar to those in the ecstasy user groups. Although these results were not statistically significant and, in contrast to DVRs, SUVs are strongly affected by alterations of local perfusion, further clarification is needed.

Concerning the tracer used in this study, ^{11}C -(+)-McN5652 has been shown to be appropriate for the quantification of SERT availability in brain regions with high SERT density, such as the mesencephalon, basal ganglia, and thalamus (7,20,21,34,35). The limitations of ^{11}C -(+)-

McN5652 are focused on its relatively high nonspecific binding and the slow kinetics.

High nonspecific binding of ^{11}C -(+)-McN5652 makes examination of SERT in regions with relatively low SERT density—such as the neocortex, for example—difficult. Therefore, these regions were not evaluated in this study.

In addition, within a reference tissue approach, high nonspecific binding of ^{11}C -(+)-McN5652 makes careful selection of an appropriate reference region necessary to estimate specific binding. In this study, according to Parsey et al. (20), the gray matter of the cerebellum was used as the reference region. The suitability of the cerebellum as the reference region is evident because of its relatively large size combined with its relatively high perfusion. This makes reproducible generation of time–activity curves with sufficient counting statistics possible. The disadvantage might be a small amount of specific tracer binding in the cerebellum (19). Alternatively, Buck et al. (21) used the white matter as the reference region. However, this may lead to increased variance and, therefore, decreased separation power. A further approach to estimate nonspecific binding is the use of the pharmacologically inactive enantiomer ^{11}C -(-)-McN5652 (7,36). This approach is controversial in recent literature. Blocking experiments revealed a significant nondisplaceable difference between the total DVs of both enantiomers (20).

The relatively slow kinetic of ^{11}C -(+)-McN5652 requires long acquisition times. In our study the acquisition time of the dynamic emission scan was limited to 90 min. A longer acquisition would be hardly acceptable for most subjects and would lead to an increased probability of motion artifacts because motion during a frame cannot be removed in sinogram mode (compared with list mode). In addition, using 2-dimensional sampling, the counting statistic is not acceptable in very late frames. According to the results of both Parsey et al. (20) and Buck et al. (21), there is no significant systematic bias of kinetic parameters at acquisition times of >80 min. However, statistical power may be limited to some extent. Parsey et al. reported a dispersion of 20% at 90-min acquisition time (dispersion = SD of distribution volume expressed as percentage of the reference value obtained with 150-min acquisition time). However, reference tissue methods are generally assumed to be less sensitive to statistical errors than complete invasive modeling (see below).

The problem of counting statistics in 2-dimensional mode acquisition at late times can be overcome by using the ^{18}F -labeled *S*-fluoromethyl analog of (+)-McN5652 (37) because of the much longer half-life of ^{18}F compared with that of ^{11}C (110 min vs. 20 min). On the other hand, the better counting statistics of the *S*-fluoromethyl analog is accompanied by an 8-fold lower binding affinity to the SERT (37). Therefore, the use of SERT radioligands developed recently, which provide both fast kinetics and low nonspecific binding, might be more appropriate.

Concerning the injected tracer mass, the number of receptors occupied by the tracer should be kept very low to fulfill the requirements of conventional modeling approaches (linear, first-order kinetics, that is, the tracer concentration available for binding should be significantly below the $K_i = 0.4$ nmol/L of unlabeled (+)-McN5652 needed to displace 5-HT from the SERT (38). Due to continuous improvements in the tracer synthesis, which resulted in permanent increase of specific activities injected, there were significant differences between the different groups regarding the amount of (+)-McN5652 injected (Table 4). This is explained by the sequence of admission of the groups to the study. On average, ecstasy users were investigated before control subjects and polydrug users. To exclude potential systematic errors due to different amounts of (+)-McN5652, linear regression analysis was performed between the DVR and the injected mass in the group of drug-naïve control subjects, which did not reveal significant correlation ($\text{DVR}[\text{mesencephalon}] = 0.0004 \times \text{injected mass [nmol]} + 1.2207$; $P[\text{slope}] = 0.72$).

Head movement minimization was achieved by a thermoplastic mask immobilization system, and the remaining head movement during the dynamic acquisition was compensated using the Realign-Tool of SPM. The maximum motion correction required was 3.4 ± 2.0 and 2.6 ± 2.5 mm in the axial and the transaxial direction, respectively. However, all correction was limited to the emission scans; subject motion between the attenuation correction scan and dynamic emission scans was not compensated. Andersson et al. (39) demonstrated that a horizontal (*x*-direction) transmission–emission mismatch of 5 mm causes errors of up to 10% in cortical regions of interest in H_2^{15}O PET studies of adult subjects. However, the effects of transmission–emission mismatch are certainly smaller in the central structures examined here and, to some extent cancel, when VOIs in both hemispheres are averaged.

There are several methods to determine the DVR of ^{11}C -(+)-McN5652 in the human brain. These methods can be divided into 2 major classes: invasive methods, which require the arterial input function; and noninvasive reference tissue methods, in which the time–activity curve of a receptor-free reference region plays the role of the input function.

In our study, the Ichise noninvasive plot was applied for the determination of the DVR of ^{11}C -(+)-McN5652. This approach yields estimates that are independent of regional cerebral blood flow and peripheral clearance of the tracer, as has been shown by simulation studies (23). In healthy volunteers, Buck et al. (21) found a high correlation of the DVR obtained from the Ichise noninvasive plot and the DV in the receptor compartment computed by application of the invasive 2-compartment model approach.

The Ichise noninvasive plot has some advantages compared with invasive methods. Acton et al. (40), who recently quantified the SERT in baboons using the new SERT SPECT ligand ^{123}I -ADAM, found that the test–retest reli-

ability was much better for the Ichise plot than for full kinetic modeling (5.4% vs. 14.5%). Therefore, small changes in SERT availability might be detected more reliably by the Ichise noninvasive plot than by application of invasive methods. This is particularly important because of the limited sensitivity of *in vivo* imaging approaches for the detection of changes of SERT. In addition, the Ichise noninvasive plot can be easily applied on a voxel-by-voxel base to generate parametric images. This allows quality control by visual inspection of the images and the application of voxel-wise statistical analysis using SPM for exploratory evaluation beyond hypothesis-driven VOI evaluation—that is, without an *a priori* selection of regions. Finally, noninvasive methods in general improve compliance of the subjects because arterial blood sampling presents a significant discomfort to most people.

The main disadvantage of the Ichise noninvasive method is the vulnerability of its DVR estimate with respect to variations of the nondisplaceable component of the tracer distribution—that is, free tracer and nonspecifically bound tracer. To attribute detected group differences to different SERT availability, it must be assumed that there is no intergroup difference of the nondisplaceable tracer distribution. To some extent this assumption is supported by the fact that there was no difference in group means of the DVR in white matter, which is devoid of SERT.

When comparing the DVR obtained in this study with previous results, it is noted that there is no consistency in the reported values of normal DVR. For example, using an invasive 1-compartment, 3-parameter model, Parsey et al. (20) found the thalamus-to-cerebellum DVR to be 1.9 and Buck et al. (21) found the ratio to be 1.8, whereas Szabo et al. (35) found the ratio to be 4.3 (the DVR was computed using uncorrected DVs from Table 2). In this study, using the noninvasive Ichise plot, the mean DVR in the thalamus was 1.4, which is lower than all of the cited values. This finding may be explained by several different factors. First, there could be a systematic underestimation of the DVR because of the use of a graphic reference tissue approach. This is supported by the results of Acton et al. (40), who found that the noninvasive Ichise plot indeed produced some bias by slightly underestimating the DVR compared with the invasive full kinetic model. Underestimation of the DVR and DVs has also been observed for graphic methods other than the Ichise noninvasive plot. In the case of the Ichise noninvasive plot, singular value decomposition of the coefficient matrix of the operational equation yields very large condition numbers. This indicates that the underestimation of the DVR is related to effects of statistical noise. Therefore, stable application of the Ichise noninvasive plot might require some kind of regularization that could be obtained by positivity constraints, for example.

A second factor causing rather low DVRs might be the reconstruction algorithm used. Parsey et al. (20) performed reconstruction by filtered backprojection (FBP), whereas in our study iterative OSEM reconstruction was used. Be-

langer et al. (41) investigated the effect of FBP versus OSEM on the binding potential of the 5-HT_{1A} receptor ligand ¹¹C-WAY-100635 computed by application of an invasive 3-compartment model in the dorsal raphe nucleus in 3 healthy volunteers. Compared with FBP, OSEM reconstruction produced a binding potential that was 28% ± 9% lower. However, this decrease in binding potential was accompanied by 17% ± 19% improvement in goodness of fit as measured by the residual sum of squares.

In addition, DVRs might be affected by the recovery effect due to the finite spatial resolution of PET. Parsey et al. (20) specified in-plane resolution of 6.0-mm FWHM at the center of the field of view. In our study, in-plane resolution was about 9-mm FWHM. Therefore, recovery effects are expected to be larger in this study and to affect all regions with at least 1 linear dimension smaller than 27 mm (3 times FWHM).

Finally, DVRs are affected by the definition of VOIs. In this study, VOIs were predefined in the template. To guarantee reproducible results no manual adjustment was performed in individual images. If VOIs are drawn manually in PET images, one tends to place the VOIs in regions with maximum tracer uptake. However, the effects of residual mispositioning of the predefined VOIs in individual PET images after stereotactic normalization were estimated by reprocessing the data with the hottest voxel analysis of large VOIs (results not shown). Large VOIs were predefined in the template such that the whole structure of interest, but no other gray matter structure, was included in the VOI. Large VOIs were then evaluated by the hottest voxel analysis (mean value of the hottest voxels), where the number of hottest voxels was taken to be the number of voxels of the corresponding small VOI composed of circles (Fig. 1). Statistical analysis of the hottest voxel data confirmed the results of the statistical analysis of the circles-VOI-data.

Neglect of the vascular contribution to time-activity curves within reference tissue methods is expected to cause only minor systematic errors.

CONCLUSION

Our findings yield further evidence for ecstasy-induced protracted alterations of the brain serotonergic system that last at least several weeks. Subjects who match ecstasy users with respect to the use of psychoactive drugs other than ecstasy, but do not use ecstasy, are more appropriate for the evaluation of ecstasy-induced long-term effects than drug-naïve control subjects. Finally, our results might indicate reversibility of the availability of SERT as measured by PET, which, however, does not imply full reversibility of neurotoxic effects. To further elucidate this question, follow-up examinations of MDMA users might be useful.

ACKNOWLEDGMENTS

We thank Prof. Dr. Jörg van den Hoff for his support in modeling. The study was supported by the Federal Institute

REFERENCES

- Burgess C, O'Donohoe A, Gill M. Agony and ecstasy: a review of MDMA effects and toxicity. *Eur Psychiatry*. 2000;15:287–294.
- Stone DM, Stahl DC, Hanson GR, Gibb JW. The effects of 3,4-methylenedioxyamphetamine (MDMA) and 3,4-methylenedioxyamphetamine (MDA) on monoaminergic systems in the rat brain. *Eur J Pharmacol*. 1986;128:41–48.
- Commins DL, Vosmer G, Virus RM, Woolverton WL, Schuster CR, Seiden LS. Biochemical and histological evidence that methylenedioxyamphetamine (MDMA) is toxic to neurons in the rat brain. *J Pharmacol Exp Ther*. 1987;241:338–345.
- Battaglia G, Yeh SY, O'Hearn E, Molliver ME, Kuhar MJ, De Souza EB. 3,4-Methylenedioxyamphetamine and 3,4-methylenedioxyamphetamine destroy serotonin terminals in rat brain: quantification of neurodegeneration by measurement of [³H]paroxetine-labeled serotonin uptake sites. *J Pharmacol Exp Ther*. 1987;242:911–916.
- O'Hearn E, Battaglia G, De Souza EB, Kuhar MJ, Molliver ME. Methylenedioxyamphetamine (MDA) and methylenedioxyamphetamine (MDMA) cause selective ablation of serotonergic axon terminals in forebrain: immunocytochemical evidence for neurotoxicity. *J Neurosci*. 1988;8:2788–2803.
- Ricaurte GA, Finnegan KT, Irwin I, Langston JW. Aminergic metabolites in cerebrospinal fluid of humans previously exposed to MDMA: preliminary observations. *Ann NY Acad Sci*. 1990;600:699–710.
- Szabo Z, Kao PF, Scheffel U. Positron emission tomography imaging of serotonin transporters in the human brain using [¹¹C](+)-McN5652. *Synapse*. 1995;20:37–43.
- McCann UD, Szabo Z, Scheffel U, Dannals RF, Ricaurte GA. Positron emission tomographic evidence of toxic effect of MDMA (“ecstasy”) on brain serotonin neurons in human beings. *Lancet*. 1998;352:1433–1437.
- Semple DM, Ebmeier KP, Glabus MF, O'Carroll RE, Johnstone EC. Reduced in vivo binding to the serotonin transporter in the cerebral cortex of MDMA (“ecstasy”) users. *Br J Psychiatry*. 1999;175:63–69.
- Buchert R, Obrocki J, Thomasius R, et al. Long-term effects of ecstasy abuse on the human brain studied by FDG PET. *Nucl Med Commun*. 2001;22:889–897.
- Obrocki J, Buchert R, Väterlein O, Thomasius R, Beyer W, Schiemann T. Ecstasy: long term effects on the human central nervous system revealed by positron emission tomography. *Br J Psychiatry*. 1999;175:186–188.
- Suehiro M, Ravert HT, Dannals RF, Scheffel U, Wagner HN Jr. Synthesis of a radiotracer for studying serotonin uptake sites with positron emission tomography: [¹¹C]McN-5652-Z. *J Labelled Compds Radiopharm*. 1992;31:841–848.
- Wittchen HU, Zaudig M. *Strukturiertes Klinisches Interview für DSM-IV (SKID I and II: Structured Clinical Interview for DSM-IV)*. Göttingen, Germany: Hogrefe; 1997.
- American Psychiatric Association. *Diagnostic and Statistical Manual of Mental Disorders*. 4th ed., text revision. Washington, DC: American Psychiatric Association; 2000.
- Schulze O, Schmidt U, Voss J, Nebeling B, Adiwidjaja G, Scharwächter K. The structure of McN-5652. *Bioorg Med Chem*. 2001;9:2105–2111.
- Mikolajczyk K, Szabatin M, Rudnicki P, Grodzki M, Burger C. A JAVA environment for medical image data analysis: initial application for brain PET quantitation. *Med Inform (Lond)*. 1998;23:207–214.
- Rorden C, Brett M. Stereotaxic display of brain lesions. *Behav Neurol*. 2001;12:191–200.
- Acton PD, Friston KJ. Statistical parametric mapping in functional neuroimaging: beyond PET and fMRI activation studies. *Eur J Nucl Med*. 1998;25:663–667.
- Laruelle M, Vanisberg M-A, Maloteaux J-M. Regional and subcellular localization in human brain of [³H]paroxetine binding: a marker of serotonin uptake sites. *Biol Psychiatry*. 1988;24:299–309.
- Parsey RV, Kegeles LS, Hwang DR, et al. In vivo quantification of brain serotonin transporters in humans using [¹¹C]McN5652. *J Nucl Med*. 2000;41:1465–1477.
- Buck A, Gucker PM, Schonbachler RD, et al. Evaluation of serotonergic transporters using PET and [¹¹C](+)-McN-5652: assessment of methods. *J Cereb Blood Flow Metab*. 2000;20:253–262.
- Weeks RA, Cunningham VJ, Piccini P, Waters S, Harding AE, Brooks DJ. [¹¹C]-Diprenorphine binding in Huntington's disease: a comparison of region of interest analysis with statistical parametric mapping. *J Cereb Blood Flow Metab*. 1997;17:943–949.
- Ichise M, Ballinger JR, Golan H, et al. Noninvasive quantification of dopamine D2 receptors with iodine-123-IBF SPECT. *J Nucl Med*. 1996;37:513–520.
- Logan J, Fowler JS, Volkow ND, et al. Graphical analysis of reversible radioligand binding from time-activity measurements applied to [¹¹C-methyl]-(-)-cocaine PET studies in human subjects. *J Cereb Blood Flow Metab*. 1990;10:740–747.
- Reneman L, Lavalaye J, Schmand B, et al. Cortical serotonin transporter density and verbal memory in individuals who stopped using 3,4-methylenedioxyamphetamine (MDMA or “ecstasy”): preliminary findings. *Arch Gen Psychiatry*. 2001;58:901–906.
- Reneman L, Booij J, de Bruin K, et al. Effects of dose, sex, and long-term abstinence from use on toxic effects of MDMA (ecstasy) on brain serotonin neurons. *Lancet*. 2001;358:1864–1869.
- Scheffel U, Szabo Z, Mathews WB, et al. In vivo detection of short- and long-term MDMA neurotoxicity: a positron emission tomography study in the living baboon brain. *Synapse*. 1998;29:183–192.
- Gerra G, Zaimovic A, Ferri M, et al. Long-lasting effects of (±)3,4-methylenedioxyamphetamine (ecstasy) on serotonin system function in humans. *Biol Psychiatry*. 2000;47:127–136.
- Hatzidimitriou G, McCann UD, Ricaurte GA. Altered serotonin innervation patterns in the forebrain of monkeys treated with (±)3,4-methylenedioxyamphetamine seven years previously: factors influencing abnormal recovery. *J Neurosci*. 1999;19:5096–5107.
- Kish SJ, Furukawa Y, Ang L, Vorce SP, Kalasinsky KS. Striatal serotonin is depleted in brain of a human MDMA (ecstasy) user. *Neurology*. 2000;55:294–296.
- Reneman L, Booij J, Schmand B, van den Brink W, Gunning B. Memory disturbances in “ecstasy” users are correlated with an altered brain serotonin neurotransmission. *Psychopharmacology (Berl)*. 2000;148:322–324.
- Reneman L, Habraken JB, Majoie CB, Booij J, den Heeten GJ. MDMA (“ecstasy”) and its association with cerebrovascular accidents: preliminary findings. *AJNR*. 2000;21:1001–1007.
- Jacobsen LK, Staley JK, Malison RT, et al. Elevated central serotonin transporter binding availability in acutely abstinent cocaine-dependent patients. *Am J Psychiatry*. 2000;157:1134–1140.
- Szabo Z, Scheffel U, Suehiro M. Positron emission tomography of 5-HT transporter sites in the baboon brain with [¹¹C]McN5652. *J Cereb Blood Flow Metab*. 1995;15:798–805.
- Szabo Z, Scheffel U, Mathews WB, et al. Kinetic analysis of [¹¹C]McN5652: a serotonin transporter radioligand. *J Cereb Blood Flow Metab*. 1999;19:967–981.
- Szabo Z, Kao PF, Mathews WB, et al. Positron emission tomography of 5-HT reuptake sites in the human brain with C-11 McN5652 extraction of characteristic images by artificial neural network analysis. *Behav Brain Res*. 1996;73:221–224.
- Zessin J, Eskola O, Brust P, et al. Synthesis of S-([¹⁸F]fluoromethyl)-(+)-McN5652 as a potential PET radioligand for the serotonin transporter. *Nucl Med Biol*. 2001;28:857–863.
- Shank RP, Vaught JL, Pelley KA, Setler PE, McComsey DF, Maryanoff BE. McN-5652: a highly potent inhibitor of serotonin uptake. *J Pharmacol Exp Ther*. 1988;247:1032–1038.
- Andersson JL, Vagnhammar BE, Schneider H. Accurate attenuation correction despite movement during PET imaging. *J Nucl Med*. 1995;36:670–678.
- Acton PD, Choi SR, Hou C, Plossl K, Kung HF. Quantification of serotonin transporters in nonhuman primates using [¹²³I]ADAM and SPECT. *J Nucl Med*. 2001;42:1556–1562.
- Belanger M-J, Parsey RV, Anderson A, Mann JJ. The effect of OS-EM versus FBP on the binding potential of the dorsal raphe nucleus in 3d-brain PET with [¹¹C]-WAY-100635 [abstract]. *J Nucl Med*. 2001;42(suppl):186P.